Mutagenesis of the Phosphatidylinositol 4,5-Bisphosphate (PIP_2) Binding Site in the NH_2-Terminal Domain of Ezrin Correlates with Its Altered Cellular Distribution

Cécile Barret,* Christian Roy,* Philippe Montcourrier,* Paul Mangeat,* and Verena Niggli‡

*Dynamique Moléculaire des Interactions Membranaires, Université Montpellier II, Unité Mixte de Recherche (UMR) Centre National de la Recherche Scientifique 5539, 34095, Montpellier Cedex 5, France; and ‡Department of Pathology, University of Bern, 3010-Bern, Switzerland

Abstract. The cytoskeleton-membrane linker protein ezrin has been shown to associate with phosphatidylinositol 4,5-bisphosphate (PIP_2)-containing liposomes via its NH_2-terminal domain. Using internal deletions and COOH-terminal truncations, determinants of PIP_2 binding were located to amino acids 12–115 and 233–310. Both regions contain a $KK(X)_nK/RK$ motif conserved in the ezrin/radixin/moesin family. K/N mutations of residues 253 and 254 or 262 and 263 did not affect cosedimentation of ezrin 1-333 with PIP_2-containing liposomes, but their combination almost completely abolished the capacity for interaction. Similarly, double mutation of Lys 63, 64 to Asn only partially reduced lipid interaction, but combined with the double mutation K253N, K254N, the interaction of PIP_2 with ezrin 1-333 was strongly inhibited. Similar data were obtained with full-length ezrin. When residues 253, 254, 262, and 263 were mutated in full-length ezrin, the in vitro interaction with the cytoplasmic tail of CD44 was not impaired but was no longer PIP_2 dependent. This construct was also expressed in COS1 and A431 cells. Unlike wild-type ezrin, it was not any more localized to dorsal actin-rich structures, but redistributed to the cytoplasm without strongly affecting the actin-rich structures. We have thus identified determinants of the PIP_2 binding site in ezrin whose mutagenesis correlates with an altered cellular localization.

Key words: cytoskeleton • actin • CD44 • A431 cells • COS1 cells

Introduction

Members of the ezrin/radixin/moesin (ERM)[1] family and the related tumor suppressor merlin are part of the protein 4.1 superfamily. They are defined as cytoskeleton-membrane linkers (for reviews, see Bretscher, 1999; Mangeat et al., 1999). The anchorage of the ERM family to the plasma membrane occurs in different ways. Indirect binding of ERM to different proteins with several transmembranous domains, such as the cystic fibrosis transmembrane conductance regulator (Short et al., 1998) or the Na^+/H^+ antiporter (Murthy et al., 1998; Yun et al., 1998), involves an adaptor protein such as EBP 50 (Reczek et al., 1997). ERM can also be linked to the cytoplasmic tail of membrane proteins with a single transmembranous domain such as CD43, CD44, I-CAM 1, I-CAM 2, and I-CAM 3. These interactions appear to be facilitated by the phospholipid phosphatidylinositol 4,5-bisphosphate (PIP_2) (Hirao et al., 1996; Serrador et al., 1997; Yonemura et al., 1998). It is not clear whether this dependency is due to a requirement for PIP_2 of the transmembranous protein or of the ERM itself (Hirao et al., 1996; Heiska et al., 1998). Some studies suggest that PIP_2 could help unmask cryptic binding sites in ERM. PIP_2 could thus be involved in the activation process of the ERM, switching the inactive "dormant" molecule to an activated state (Matsui et al., 1999; Nakamura et al., 1999). ERM could also directly interact with PIP_2-containing phospholipid bilayers (Niggli et al., 1995; Hirao et al., 1996; Heiska et al., 1998). Thus, the direct association of ezrin with PIP_2 and also with the p85 subunit of the phosphatidylinositol 3-kinase may provide a mechanism to anchor the enzyme in proximity to its substrate (Gautreau et al., 1999).

Talin, another member of the 4.1 family, has been shown to insert into bilayers of liposomes containing acidic phospholipids using hydrophobic photolabeling. Lipid interaction was attributed to a 47 kD NH_2-terminal domain (Niggli et al., 1994). Similarly, we have demonstrated that the NH_2-terminal domain of ezrin (amino acids 1–309) was

Address correspondence to Verena Niggli, Dept. of Pathology, University of Bern, Murtenstr. 31, P.O. Box 62, CH-3010 Bern, Switzerland. Tel.: 41 31 632 87 44. Fax: 41 31 381 34 12. E-mail: niggli@patho.unibe.ch

[1]*Abbreviations used in this paper:* ERM, ezrin/radixin/moesin; GST, glutathione S-transferase; PH, pleckstrin homology; PIP_2, phosphatidylinositol 4,5-bisphosphate; PC, phosphatidylcholine; VSV-G, vesicular stomatitis virus glycoprotein G.

necessary and sufficient for interaction with PIP_2-containing liposomes. We showed that ezrin binds preferentially to liposomes containing PIP_2 as compared with other phospholipids such as phosphatidylserine, and that this interaction occurs at physiological ionic strength. Under these conditions, ezrin discriminates between PIP_2, phosphatidylinositol 4-monophosphate, and phosphatidylinositol (Niggli et al., 1995).

In this study, we further characterized the interaction of the NH_2-terminal domain of ezrin with PIP_2-containing liposomes by truncation and site-directed mutagenesis. Amino acids that are involved in binding to PIP_2-containing liposomes have been identified. They are located in two distinct regions of this domain. Similarly, PIP_2 interaction was abolished when the same critical mutations were introduced in the full-length ezrin molecule. Although the PIP_2-independent interaction of ezrin with proteins was not affected, its intracellular localization was drastically changed. Expression of the mutated first 310 amino acids of ezrin led to a loss of the ability of the NH_2-terminal domain of ezrin to promote cell extensions (Martin et al., 1997; Amieva et al., 1999).

Materials and Methods

Site-directed Mutagenesis

The preparation of constructs with internal deletions as well with COOH-terminal truncations has already been described (Roy et al., 1997). The numbering of the amino acid sequence of ezrin includes the first methionine, corresponding to the protein expressed in bacteria. The quick change site-directed mutagenesis kit from Stratagene was used. The changed bases are underlined. The oligonucleotides (sense) (5′–3′) used for introducing the K63N mutation in pGEX-2T ezrin 1-586 were GGCTGAAGCTGGATAATAAGGTGTCTGCCCAGG (12 cycles, 95°C, 30 s; 55°C, 1 min; 68°C, 15 min) and GGAACATCTCTTTCAATGACAATAATTTTGTCATTAAACCC for K253N, K254N (16 cycles, 95°C, 30 s; 50°C, 1 min; 68°C, 14 min). The following oligonucleotides were used to mutate the pGEX-2T ezrin 1-333: GGCTGAAGCTGGATAATAATGTGTCTGCCCAGGAGG (K63N, K64N), GTCATTAAACCCATCGACAATAATGCACCTGACTTTGTG (K262N, K263N) and GCTGGATAAGAAGGTGGCTGCCCAGGAGGTCAGG (S66A). For this later series, 14 cycles were performed (95°C, 30 s; 55°C, 1 min; 68°C, 12 min). The K63N mutation was introduced in the pGEX-2T ezrin 1-333 vector by excising the XmaI/AatII fragment of pGEX ezrin 1-333 and cloning this fragment in the pGEX-2T ezrin 1-586 K63N deleted from its XmaI/AatII fragment. The K253N, K254N, K262N, and K263N mutations were introduced in the pGEX-2T ezrin 1-333 K63,64N vector after purification of the inserts Cfr9I/KpnI containing the indicated mutations. The K253N, K254N, K262N, and K263N mutations were introduced in pGEX-2T ezrin 1-586 after excising the Asp718/Cfr9I fragment from pGEX-2T ezrin 1-333 and ligation in the similarly cut recipient vector. The K63N, K64N, K253N, K254N, K262N, and K263N mutations from pGEX-2T ezrin 1-333 K63N, K64N, K253N, K254N, K262N, and K263N were introduced in pGEX-2T ezrin 1-586 after excising the NcoI/Cfr9I fragment. For transfection experiments, the K253N, K254N, K262N, and K263N mutations were introduced into the pCB6 vesicular stomatitis virus glycoprotein G (VSV-G)–tagged plasmid encoding for the wild-type ezrin, a kind gift of Dr. Monique Arpin (Curie Institute, Paris, France) (Algrain et al., 1993). The similarly mutated ezrin 1-310 tagged with the VSV-G peptide was derived from the above construct using appropriate restriction enzymes. All constructs were sequenced using the T7 Sequenase version 2.0 (Amersham Pharmacia Biotech).

Plasmid (pSR CD44) encoding the full-length CD44 protein was obtained from R. Lamb (MRC, London, UK). The region coding for the cytoplasmic tail of the protein (amino acids 291–360) was amplified by polymerase chain reaction using the Pfu polymerase (Stratagene) and subcloned in the BamHI/EcoRI site of the pGEX-2T vector. The vector encoding the amino acids 329–358 of EBP50 in fusion with glutathione S-transferase (GST) was provided by A. Bretscher (Cornell University, Ithaca, NY).

Protein Expression and Purification

After an overnight culture in LB medium (Luria Broth) at 37°C, protein expression was induced with 0.5 mM isopropyl β-D-thiogalactopyranoside for 45 min (NH_2-terminal constructs) or 1 h (full-length ezrin). The following conditions are given for a 1 liter culture scale and all steps were performed at 4°C. Bacteria were pelleted at 5,000 *g*, resuspended in 15 ml PBS containing protease inhibitors (Complete; Boehringer) and sonicated three times for 2 min with pulses for 50% of the time. The sonicated bacteria were diluted to 30 ml with PBS, centrifuged for 30 min at 17,000 *g*, and the supernatant was diluted to 50 ml. Glutathione-agarose (1.5 ml gel) was added to the supernatant and left on a rotary shaker. For NH_2-terminal constructs, fusion proteins were allowed to adsorb on the gel overnight. The slurry was then poured in a column and washed with PBS. Further washing of the column was carried out with Tris-HCl, pH 7.4, and 100 mM NaCl. Nucleic acids bound on the fusion protein were then degraded by adding 150 U benzonase and 50 μg RNase after an incubation at room temperature for 90 min. After washing the column, the same buffer, but containing 2.5 mM $CaCl_2$, was added together with 5 IU thrombin and the cleavage was allowed to process for 90 min. The protein was recovered in the eluate and the thrombin action was stopped with para-aminobenzamidine beads (Sigma-Aldrich).

For full-length ezrin constructs, the fusion proteins were allowed to adsorb on the glutathione agarose gel for 2 h. The gels were poured in a column and washed sequentially with PBS and Tris-HCl, pH 8.0. After glutathione elution (10 mM), full-length ezrin was dialyzed overnight against a buffer containing 20 mM Tris-HCl, pH 7.4, 0.1 mM EDTA, and 15 mM mercaptoethanol. 50 mM NaCl and 2.5 mM $CaCl_2$ were added to the dialysate. Digestion with thrombin was allowed to proceed for 90 min at 37°C. Samples were diluted twice with FPLC buffer A (25 mM MES, pH 6.2, 20 mM NaCl, and 0.01% mercaptoethanol). Elution from the mono-Q column of wild-type ezrin as well as of ezrin with mutations K253N, K254N, K262N, and K263N occurred at 65 mM NaCl, that of ezrin with mutations K63N, K64N, K253N, K254N, K262N, and K263N at 85 mM NaCl. All proteins were stored at 4°C in the presence of 0.05% NaN_3.

The cytoplasmic tail of CD44 and the EBP50 fragment were obtained using procedures similar to that used for ezrin full-length constructs, except that the fusion proteins were not eluted from the glutathione agarose gel. The adsorbed GST-CD44 protein was kept at 4°C and used within 24 h after preparation.

Determination of Protein Concentration

The UV spectra were recorded and the protein concentration was calculated from the absorption coefficients at 220 and 280 nm. The Bradford assay (Bradford, 1976) did not allow a quantitative estimation of the protein content because of the peculiar amino acid composition of the NH_2-terminal constructs; this assay was used only for comparing relative amounts of the protein.

Phospholipids

Phosphatidylcholine (PC) and PIP_2 were obtained from Lipid Products. For some experiments, PIP_2 was also obtained from Sigma-Aldrich. No difference was detected between the two products.

Cosedimentation of Ezrin and Ezrin Constructs with Lipid Vesicles

Analysis of protein–lipid interactions by cosedimentation of proteins with large multilamellar liposomes has been documented in detail elsewhere (Niggli et al., 1994). Large, multilamellar liposomes were prepared from PC and PIP_2 in a buffer containing 20 mM Hepes, pH 7.4, 0.2 mM EGTA as described (Niggli et al., 1995). Ezrin, and ezrin constructs (dialyzed after purification against a buffer containing 20 mM Tris/HCl, pH 7.4, 0.1 mM EDTA, 15 mM mercaptoethanol) were centrifuged before the experiments for 20 min at 20,000 *g*, 4°C, followed by protein determination. Proteins were subsequently incubated for 15 min at 22°C in the presence of 130 mM KCl and in the absence of liposomes, followed by a further incubation in the absence or presence of liposomes for 15 min. In part of the experiments, proteins were not dialyzed after purification, and lipid interactions of ezrin constructs were assayed directly in the buffer in which the protein was recovered after column chromatography. In this case, EGTA was added to the protein solution to neutralize Ca^{2+}, which interferes with the liposome cosedimentation assay (see Results). This resulted in a protein solution containing (mM): 50 Tris/HCl, pH 7.4, 100 NaCl, 1.25 $CaCl_2$, 2.8 EGTA, and 0.05% NaN_3. No difference in lipid interaction of the same preparation of wild-type ezrin domains could be detected when proteins were added to the lipids before or after dialysis provided that Ca^{2+} was neutralized by EGTA. Proteins were kept under nitrogen during incubation with lipids. Final concentrations of protein were 27.5–55 μg/ml and of

lipid 0.5 mg/ml. The fraction of wild-type ezrin (1-333) cosedimenting with PIP_2-containing liposomes was similar for both protein concentrations. The mixtures were subsequently centrifuged for 30 min at 100,000 *g*, 4°C. The pellets were solubilized in 50–100 μl sample buffer (Niggli et al., 1994). The supernatants were mixed with the corresponding amount of the threefold concentrated sample buffer. After heating the samples for 5–10 min at 95°C, they were applied to SDS-polyacrylamide gradient gels (Niggli et al., 1995). The amount of protein present in pellets and supernatants was quantified by scanning the bands of the Coomassie blue-stained gels. The amount of ezrin sedimented in the absence of liposomes was always subtracted from that sedimenting in the presence of lipid (= specific cosedimentation). In a series of representative experiments, 22 ± 8% (n = 10) of wild-type ezrin 1-333 sedimented in the absence of lipid. Comparable data were obtained for mutated proteins. The amount of wild-type ezrin 1-333 recovered in the pellet was increased in the presence of liposomes containing 20% PIP_2 to 77 ± 9% (n = 10) of total protein. The specific cosedimentation of wild-type ezrin 1-333 corresponds thus to 300 ± 160% (n = 10) of the amount of protein sedimenting in the absence of lipid. Some variations were observed in the extent of cosedimentation with liposomes when comparing different protein preparations, possibly due to variable denaturation during purification and/or storage.

The data are given as mean ± SD of n experiments. Differences between data were analyzed with the Student's t test for paired data, with a $P < 0.05$ considered significant.

Interaction of Ezrin with the Cytoplasmic Tail of CD44

GST or GST-CD44 (5 μg, 10 μl) bound to glutathione agarose beads were equilibrated in the reaction buffer (25 mM Tris-HCl, pH 7.4, 150 mM KCl, 1 mM $MgCl_2$, and 1 mM DTT). PIP_2 was added in micellar form (Hirao et al., 1996). Full-length wild-type ezrin or ezrin K253N, K254N, K262N, and K263N (3.5 μg, 1 μM) were incubated in a final volume of 50 μl with beads for 1 h at room temperature. Beads were then washed three times with 500 μl buffer at 4°C. After the final wash, 20 mM glutathione was added for 1 h. Aliquots of the supernatant were then analyzed by SDS-PAGE and Western blotting for the presence of ezrin using procedures described in Roy et al. (1997).

Homotypic Interaction Assay

Wild-type ezrin 1-586 was coated in wells of a microtiter plate and residual binding sites saturated with 2% bovine serum albumin (Roy et al., 1997). Ezrin 1-333 constructs (0.5 μM each) were then added in buffer (20 mM Tris-HCl, pH 7.4, 5 mM $MgCl_2$, 100 mM KCl, and 0.2 mM dithiothreitol). After 1 h of incubation, wells were rinsed with the same buffer and samples were processed for SDS-PAGE analysis and Western blotting.

Intrinsic Tryptophane Fluorescence Measurements

Fluorescence spectra were recorded with an Aminco-Bowman Series 2 luminescence spectrometer at 30°C. Protein samples were incubated in 50 mM Tris-HCl, pH 7.4, 100 mM NaCl. The tryptophane emission fluorescence spectrum was recorded by excitation at 292 nm. Both excitation and emission beams were set at 2-nm bandwidth.

Cell Culture and Transient Transfection

COS1 and A431 cells were maintained in DMEM containing 10% FBS. Cells were seeded 24 h before transfection at a density of 200,000 cells per 35-mm dish. Transfection of plasmids into COS1 cells was carried out by using Effectene (Qiagen) as recommended by the manufacturer (0.4 μg plasmid in 100 μl EC buffer and 3.2 μl enhancer for 5 min at room temperature, then addition of 10 μl Effectene followed by contact with cells 10 min later). Superfect (QIAGEN) was used for transfection of A431 cells: 2 μg DNA was mixed with 100 μl DMEM and 10 μl Superfect for 5 min at room temperature before addition to cells. The medium was changed 3 h later. Immunofluorescence and cell fractionation were carried out 30 and 42 h after transfection, respectively.

Cell Fractionation

The cells were washed twice with PBS with 0.5 mM $MgCl_2$ and 2 mM $CaCl_2$. Lysis buffer [(mM) 10 Hepes, pH 7.4, 2.5 $MgCl_2$, 1 EGTA, 1 EDTA, 1 vanadate, 10 NaF, 0.1 PMSF, 100 μg/ml CHAPS, 10% glycerol, and a cocktail of antiproteases] was added (300 μl per 35-mm dish). Cells were scraped off with a rubber policeman and homogenized by 20 strikes in a Dounce homogenizer (pestle B). The homogenates were centrifuged at 25,000 *g* for 30 min at room temperature. The supernatant corresponds to the cytosolic fraction. The pellet was resuspended in 300 μl buffer A [(mM) 50 MES, pH 6.4, 2.5 $MgCl_2$, 1 EGTA, 1 vanadate, 10 NaF, 10% glycerol, 0.5% Triton X-100, antiprotease cocktail] and centrifuged at 18,000 *g* for 15 min at 4°C. The pellet (Triton X-100 nonextractable material) was resuspended in 300 μl buffer A and sonicated. Fractions (30 μl) were applied to SDS-polyacrylamide gels and immunoblotted with P5D4 anti–VSV-G mAb or anti-ezrin antibodies (Andréoli et al., 1994; Roy et al., 1997). Anti-ezrin antibodies generated either against the full-length protein or the first 310 residues were defined as anti–C and –N antibodies, respectively (Andréoli et al., 1994).

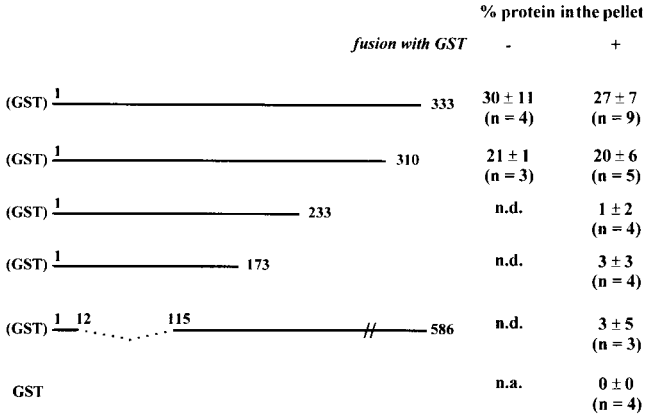

Figure 1. Effects of truncations and internal deletions on the cosedimentation of the NH_2-terminal domain of ezrin with PIP_2-containing liposomes. The cosedimentation of ezrin domains, with or without the GST moiety (55 μg protein/ml), with large liposomes containing 20% PIP_2 and 80% PC (0.5 mg lipid/ml) in the presence of 130 mM KCl was determined as described in Materials and Methods. n.d., not done; n.a., not applicable.

Immunofluorescence Analysis

Cells were fixed with 3.7% formaldehyde in PBS for 20 min and treated with TBS containing 0.2% Triton X-100 for 4 min. Cells were incubated with anti–VSV-G mAb (clone P5D4; Kreis, 1986) for 1 h at room temperature, washed, and incubated with FITC-conjugated phalloidin and Texas red–conjugated anti–mouse Ig Ab (Sigma-Aldrich). After final washes and mounting in Mowiol, cells were examined using a laser scanning confocal microscope (Leica or Bio-Rad Laboratories) using a 63× 1.4 oil immersion objective.

Results

Mapping of the PIP_2 Binding Site

Association of ezrin with the lipid bilayer was first studied with fusion proteins corresponding to the NH_2-terminal domain of ezrin, a region which has been previously shown to mediate the interaction of ezrin with PIP_2-containing liposomes (Niggli et al., 1995). As a measure for bilayer association, cosedimentation of proteins with large liposomes containing 20% PIP_2 and 80% PC was analyzed. Control values of protein sedimenting in the absence of lipid were always subtracted. Lipid interactions were measured under physiological ionic strength conditions. We have found previously that addition of 1 mM $MgCl_2$ (in the presence of 60 μM EGTA and 50 μM EDTA) markedly reduced cosedimentation of wild-type full-length ezrin with PIP_2-containing liposomes by 40–70% (data not shown). According to Flanagan et al. (1997), divalent cations promote fusion of PIP_2 micelles into insoluble aggregates and may thus also adversely affect PIP_2-containing liposomes. All the experiments were therefore carried out in the absence of added divalent cations.

POTENTIAL PIP_2 BINDING SITES

ezrin	58	WLKLD**KK**VSAQEV**RK**	72
radixin	58	WLKLN**KK**VTQQDV**KK**	72
moesin	58	WLKLN**KK**VTAQDV**RK**	72
merlin	75	WLKMD**KK**VLDHDVS**K**	89

ezrin	242	WSEIRNISFND**KK**FVI**K**PID**KK**	263
radixin	242	WSEIRNISFND**KK**FVI**K**PID**KK**	263
moesin	242	WSEIRNISFND**KK**FVI**K**PID**KK**	263
merlin	259	WNEIRNISYSD**K**EFTI**K**PLD**KK**	280

Figure 2. Potential PIP_2 binding sites in the ERM family. Sequences were obtained from the Swiss Protein data bank. Accession numbers are: ezrin, P15311; radixin, P35241; moesin, P26038; and merlin, P35240.

Progressive deletions from the COOH terminus of ezrin 1-333 illustrated the importance of amino acids 233–310 in the assay of cosedimentation with liposomes (95 ± 8% inhibition of cosedimentation for ezrin 1-233, $n = 4$; Fig. 1). The internal deletion of residues 13–114 also led to a dramatic loss of the resulting construct to interact with liposomes (89 ± 18% inhibition, $n = 3$). GST alone did not cosediment with the liposomes and elimination of the GST moiety did not affect association with PIP_2-containing liposomes (Fig. 1). This finding shows that unspecific trapping of protein in the lipid pellet is negligible under our experimental conditions. The results shown in Fig. 1 also demonstrate that ezrin 1-333 is capable of recruiting a protein incapable of membrane interaction (GST) to the bilayer. The PIP_2 binding domain of ezrin therefore appears to consist of nonlinear determinants and involves distinct portions of the molecule.

By analogy with several PIP_2-binding proteins and pleckstrin homology (PH) domains, it was inferred that a number of basic residues could be involved in such an interaction. Typical PIP_2-binding motifs consist of clusters of basic amino acids; e.g., (K/R)XXXKX(K/R)(K/R) in gelsolin or (K/R)XXXX(K/R)(KR) in villin (Janmey et al., 1992; Yu et al., 1992). Two similar motifs are conserved in the entire ERM family at identical positions and also at comparable positions in merlin, if one takes into account the extended NH_2 terminus of merlin (Fig. 2). A third motif (RXRXXRR) as well as a cluster of basic amino acids (RRRK) are present in the ERM family at positions 273–279 and 293–296, respectively. However, we demonstrate below that the two motifs shown in Fig. 2 are crucial for PIP_2 interaction. Interestingly, one of these motifs was present in the 234–309 region and one in the 13–114 portion of the molecule, the two regions identified by truncation experiments as important for PIP_2 interaction. As shown in Fig. 1, interaction with PIP_2-containing liposomes was abolished when either of these regions was deleted. The COOH-terminal domain of ezrin also contains regions with clusters of basic amino acids. However, we have shown previously that this domain does not significantly interact with PIP_2-containing liposomes (Niggli et al., 1995). These motifs thus are not functionally relevant for lipid interaction.

Table I. Effects of K to N Mutations on Cosedimentation of Ezrin 1-133 with PIP_2-containing Liposomes

Mutations K > N introduced in positions:			Percent protein in pellet	n
63 and 64	253 and 254	262 and 263		
−	−	−	59 ± 13	11
+	−	−	27 ± 4	3
+	+	−	9 ± 2	3
−	+	−	61 ± 12	6
−	−	+	48 ± 18	6
−	+	+	6 ± 4	6
+	+	+	10 ± 5	3

Wild type and mutant ezrin 1-333 domains (27.5–55 μg protein/ml) were incubated in the presence of 100 mM NaCl and in the absence or presence of large liposomes containing 20% PIP_2 and 80% PC (0.5 mg lipid/ml), followed by determination of the fraction of liposome-associated protein, as described in Materials and Methods. Mean ± SD of n experiments.

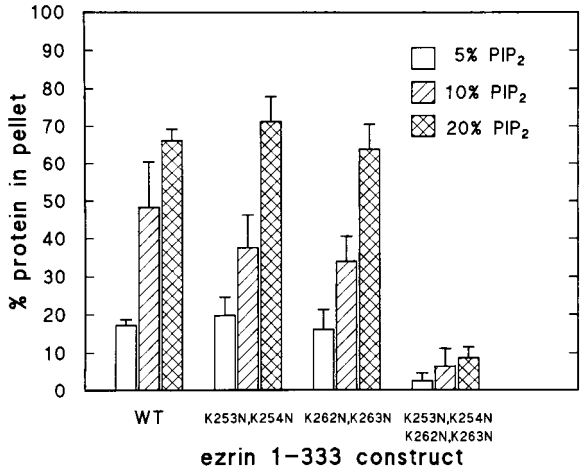

Figure 3. Cosedimentation of wild-type and mutant ezrin 1-333 with large liposomes containing different amounts of PIP_2. Wild-type (WT) and mutant ezrin domains (55 μg protein/ml) were incubated in the presence of 100 mM NaCl and in the absence or presence of large liposomes containing 5, 10, or 20% of PIP_2, the remainder being PC (0.5 mg lipid/ml). The fraction of cosedimenting protein was assessed as described in Materials and Methods. Mean ± SD of three to eight experiments.

Site-directed Mutagenesis of Potential PIP_2 Binding Sites

Several double mutations of the lysine residues located in the presumed motifs were introduced in the ezrin 1-333 molecule. As shown in Table I, double mutations of either lysines 253 and 254, or lysines 262 and 263 to asparagine did not significantly impair the ability of the mutated construct to cosediment with PIP_2-containing liposomes. The double substitution K63N, K64N by contrast led to a significant ($P < 0.025$) partial reduction in the amount of mutated ezrin 1-333 that cosedimented suggesting a particularly important role of these residues (Table I). The combination of the K253N, K254N and the K262N, K263N mutations led to an almost complete loss of interaction with PIP_2 (84 ± 11% inhibition, $n = 6$). The combination of K63N, K64N and K253N, K254N mutations resulted similarly in a protein with strongly reduced PIP_2-binding capacity (78 ± 11% inhibition, $n = 3$), far exceeding the effect of the double mutation of K63N, K64N alone. The introduction of the K262N, K263N mutations into this mutant did not further reduce binding. For optimal binding, the presence of either

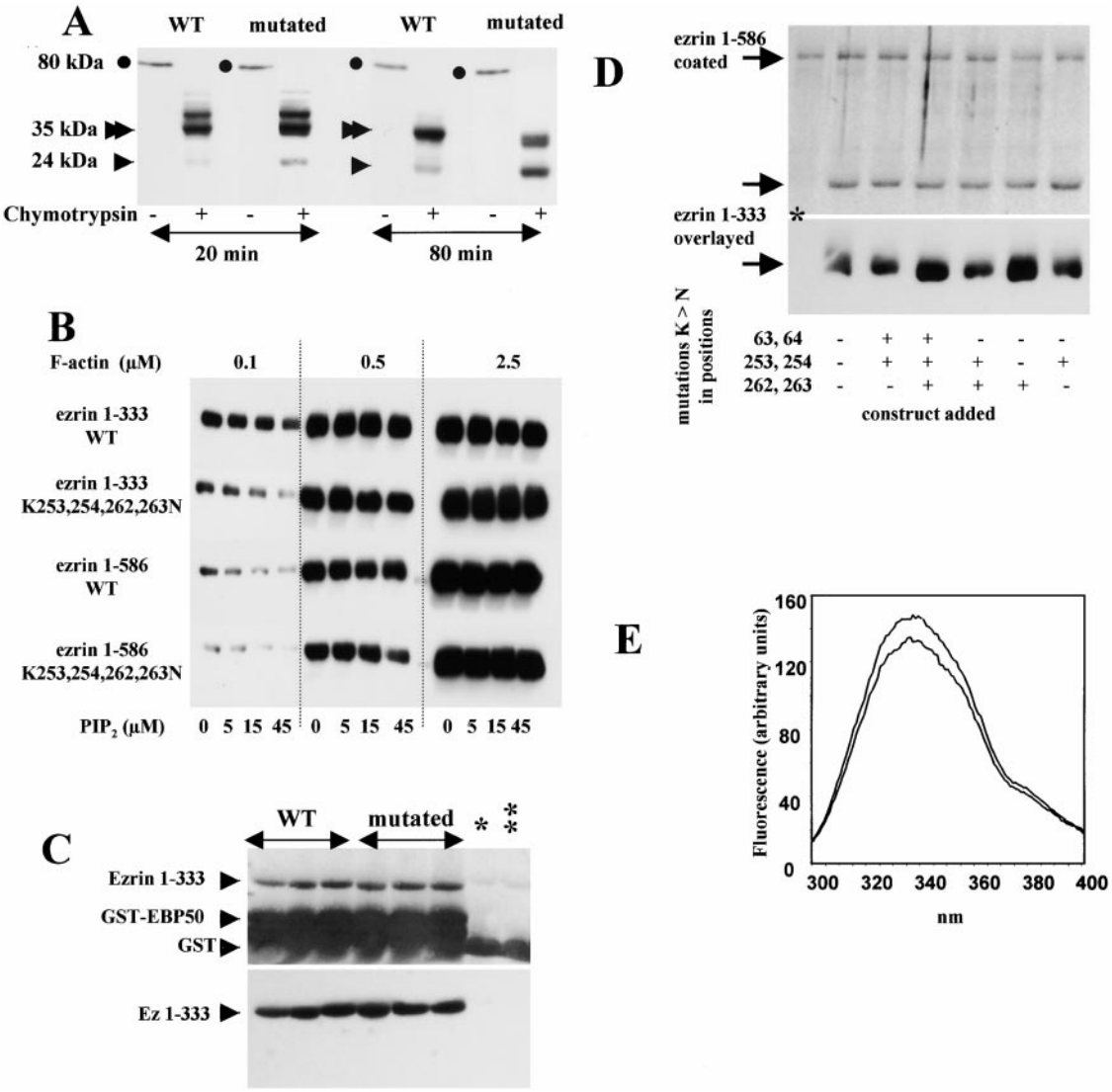

Figure 4. The mutations introduced specifically target ezrin-PIP_2 interactions. (A) Introduction of four K > N mutations in ezrin did not change the chymotrypsin digestion pattern. Wild-type (WT) and mutated ezrin 1-586 (K253N, K254N, K262N, and K263N) (285 μg/ml) were incubated in the presence or absence of 3.3 μg/ml chymotrypsin at room temperature for the indicated times. After SDS-PAGE, membranes were immunoblotted with a polyclonal antibody targeted against the first 310 amino acids of ezrin. No major difference in the digestion patterns was observed when wild-type or mutated ezrin were compared. (B) Introduction of four K > N mutations in ezrin (K253N, K254N, K262N, and K263N) did not alter F-actin binding. F-actin binding was measured using a solid phase assay as described by Roy et al. (1997). Actin concentrations were chosen so that they were below, around, and above the dissociation constant (500 nM) for actin binding to ezrin. For each actin concentration, binding was measured in the presence or absence of PIP_2. Bound actin was detected using a monoclonal anti-actin antibody. The top two blots illustrate the binding of actin to the NH_2-terminal domain of wild-type and mutant ezrin (residues 1–333). The bottom two blots correspond to actin binding to full-length ezrin with or without the four K > N mutations. No obvious difference in F-actin binding capacity was observed when comparing mutated ezrin constructs with their parent wild-type counterparts. (C) Mutagenesis of the PIP_2 binding site in ezrin 1-333 did not impair the interaction of the NH_2-terminal domain of ezrin with the cytoplasmic tail of EBP50. The binding of wild-type ezrin 1-333 (WT and *) or mutated ezrin 1-333 (mutated and **) (1 μM) to GST-EBP 50 or GST was assessed as described for binding to CD44 in Materials and Methods. (Top) Coomassie staining, (bottom) Western blotting. The experiment had been done in triplicate for each construct. Western blotting showed that there was no major difference between WT ezrin 1-333 and the mutated form concerning binding to GST-EBP50. The right two lanes demonstrate the lack of binding of ezrin 1-333 WT (*) or mutated (**) when assayed with the control GST free of fusion protein. (D) Introduction of up to six K > N mutations in ezrin did not affect homotypic interactions. Wild-type ezrin 1-586 was coated in wells of a microtiter plate (Roy et al., 1997). Ezrin 1-333 constructs (0.5 μM each) were then added in F-actin buffer, except for the first lane, where no construct was added (*). Similar amounts of ezrin 1-586 were coated in each well as judged by the Coomassie stain of the top blot. The same polyclonal anti-ezrin antibody as in A was used to detect the construct overlaid and, irrespective of the mutations introduced, no major difference in the amount of ezrin 1-333 construct bound to ezrin 1-586 was observed (bottom). When no ezrin 1-586 was coated, no ezrin 1-333 was detectable (not shown). (E) Intrinsic tryptophane fluorescence was not modified upon introduction of four K > N mutations in full-length ezrin. (Top curve) Full-length mutated ezrin K253N, K254N, K262N, and K263N; (bottom curve) wild-type ezrin 1-586. Note that neither the maximum intensity of tryptophane fluorescence nor the wavelength for maximum emission were significantly affected upon introduction of the four mutations.

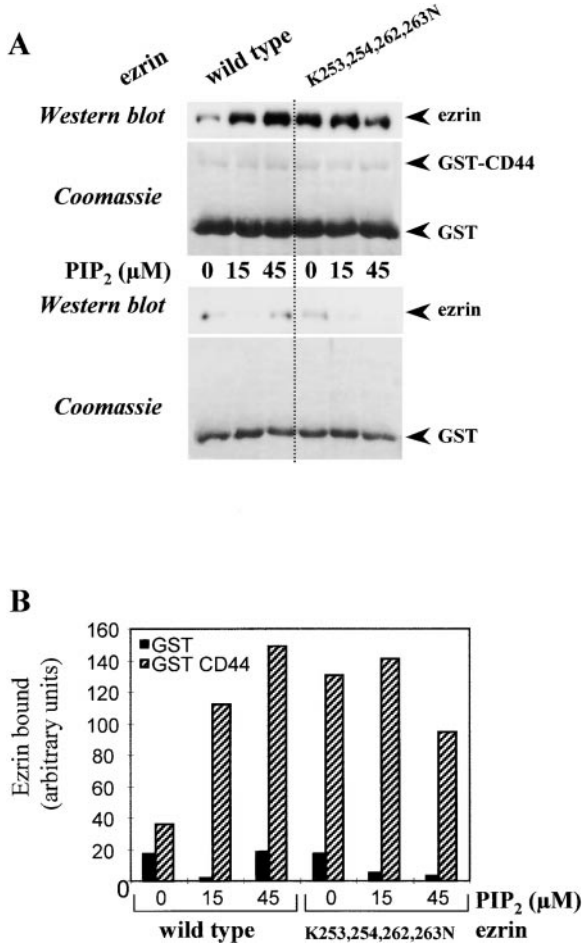

Figure 5. Mutagenesis of the PIP_2 binding site in ezrin results in a loss of PIP_2 requirement of the interaction of ezrin with the cytoplasmic tail of CD44. Binding of full-length wild-type ezrin or ezrin K253N, K254N, K262N, and K263N (K253,254,262,263N) to GST or GST-CD44 in the absence or presence of PIP_2 was assessed as described in Materials and Methods. Aliquots of the supernatant were then analyzed by SDS-PAGE and immunoblotted for the presence of ezrin. (A) Coomassie blue staining of the blots shows that comparable amounts of GST-CD44 (or GST) were detected in all lanes (top, incubation with GST-CD44 beads; bottom, incubation with GST beads). In contrast to wild-type (WT) ezrin (top left), K253N, K254N, K262N, and K263N (K253,254,262,263N) mutations in ezrin induced constitutive binding to GST-CD44–coupled agarose beads independently of the addition of PIP_2 micelles (top right). GST beads alone (bottom) were used as control. During the GST-CD44 preparation, significant cleavage of the fusion protein occurred, resulting in large amount of GST adsorbed on the gel. (B) The amount of wild-type or mutated ezrin bound to GST-CD44 or to GST alone was quantified by densitometry of the immunoblots shown in A. Black and hatched columns represent ezrin bound to GST and GST-CD44, respectively. The results shown are representative of three independent experiments.

lysines 63, 64, 253, and 254 or lysines 253, 254, 262, and 263 is thus required. The presence of lysines 63 and 64 alone is not sufficient to maintain binding, correlating with the experiments on the truncated NH_2 terminus (Fig. 1).

The finding that some double mutations (K253N, K254N or K262N, K263N) did not significantly alter PIP_2 binding of ezrin 1-333 could be due to the use of saturating amounts of PIP_2 in the liposomes, which may not allow us to detect subtle changes in lipid binding. According to our previous findings, the interaction of full-length wild-type ezrin with liposomes is maximal at 20% PIP_2 and 80% PC (Niggli et al., 1995). We therefore compared interactions of mutated and wild-type proteins with liposomes containing lower amounts of PIP_2. As shown in Fig. 3, at 10 and 5% PIP_2, no statistically significant difference was detectable between cosedimentation of mutants ezrin 1-333 K253N, K254N, ezrin 1-333 K262N, K263N, and the wild-type form of ezrin 1-333.

Since the serine 66 residue corresponds to a potential protein kinase A phosphorylation site, we performed a S66D mutation in ezrin 1-333 to analyze the effects of introducing a negative charge next to the neighboring lysine residues involved in PIP_2 binding. However, the S66D mutant behaved as the wild-type domain (not shown). Introduction of a negative charge next to lysines 63 and 64 thus does not disturb PIP_2 binding.

On the basis of the findings summarized in Fig. 1 and Table I, the full-length ezrin molecule was mutated in positions 253, 254, 262, and 263 and in combination with positions 63 and 64. The amount of mutated construct recovered in the liposome-containing pellet corresponded to 2% of total protein for K253N, K254N, K262N, and K263N and to 3% for K63N, K64N, K253N, K254N, K262N, and K263N, as compared with 24% of wild-type ezrin cosedimenting with liposomes ($n = 2$). PIP_2 interaction of these two mutants was thus almost completely abolished, corresponding to the findings with the 1-333 constructs.

Conformation and Functional Properties of Mutated Ezrin

To exclude that our findings were due to an unstable folding and/or overall denaturation of the mutated protein, we compared the sensitivity of wild-type ezrin and ezrin K253N, K254N, K262N, and K263N to chymotrypsin (Fig. 4 A). Chymotrypsin has been previously used to partially proteolyze ezrin and identify a chymotryptic-resistant NH_2-terminal domain (Franck et al., 1993; Niggli et al., 1995). No major differences in the degradation patterns were observed when ezrin was mutated: the 35- and 24-kD bands detected with an antibody directed against the first 310 amino acids of ezrin were the major degradation products for both the wild-type and the mutated ezrin, indicating therefore that both molecules were similarly folded (Fig. 4 A). However, the 24-kD degradation product appeared earlier with ezrin K253N, K254N, K262N, and K263N, suggesting that its folding was less stable than that of wild-type ezrin.

The same mutations also did not alter the ability of the full-length ezrin molecule nor that of the ezrin 1-333 construct to bind to F-actin at relatively high concentrations (0.5–2.5 μM F-actin) as measured in the solid phase assay (Fig. 4 B) (Roy et al., 1997). Under more stringent conditions (0.1 μM F-actin), the binding capacity of mutated molecules may be lowered. The addition of PIP_2 was without effect on the F-actin binding of both constructs whether they were mutated or not, emphasizing therefore the lack of requirement for PIP_2 to bind to F-actin under our assay conditions. The K253N, K254N, K262N, and K263N ezrin 1-333 also interacted with the cytoplasmic tail (amino acids 329–358) of EBP 50 in fusion with GST to the same extent as wild-type ezrin 1-333 (Fig. 4 C). No interaction with control GST was detectable.

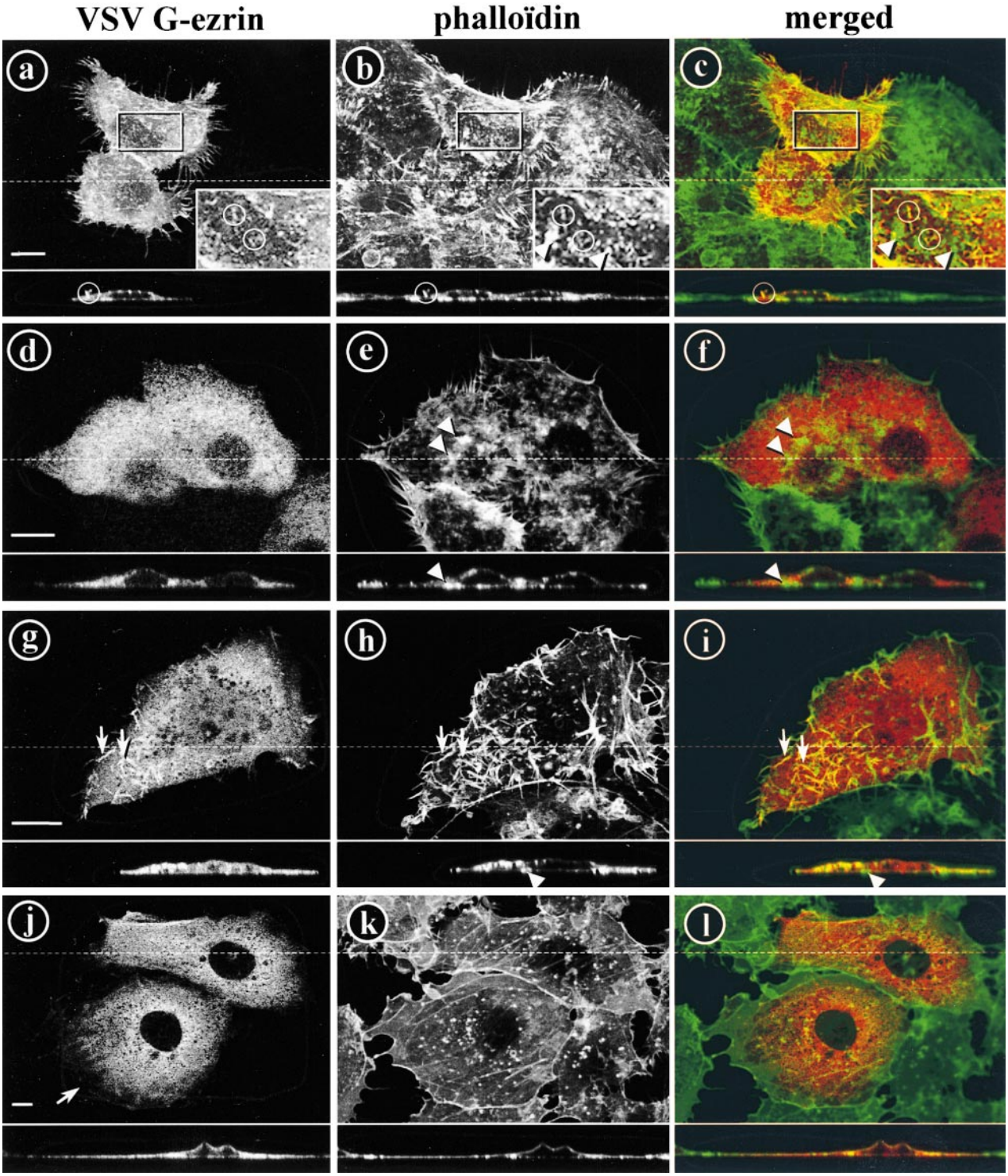

Figure 6. Mutated ezrin loses its cell membrane localization in transfected A431 and COS1 cells. Human adenocarcinoma A431 epithelioid cells (a–f) and monkey kidney COS1 fibroblasts (g–l) were transfected with either VSV-G–tagged wild-type ezrin (a–c and g–i) or mutated ezrin (K253N, K254N, K262N, and K263N) (d–f and j–l) DNA and treated for indirect Texas red localization of ezrin with anti–VSV antibody (left) and F-actin with FITC-coupled phalloidin (middle). Pictures represent the projected maximum intensities of several focal planes ranging from substrate to apical level, except for d and j. Vertical xz sections at the level of the dotted lines are under each figure. Insets are enlargements of the squared areas in a–c. Dual localizations of ezrin and actin are merged in color, colocalization appearing in yellow. Transfected wild-type ezrin is located in actin-rich cell surface structures such as microspikes, dorsal microvilli (a–c, circles) or ruffles (g–i, arrows), and in lateral cell membranes (a and c, intercellular contacts). Note that focal adhesion plaques (b, c, e, and f, insets, arrowheads) and stress fibers (k) are devoid of any ezrin. Transfected mutated ezrin is essentially located as a cytosolic network (d, f, j, and l; note that single focal planes are used only in d and j for clearer visualization of ezrin), but is also faintly detectable on the cell membranes in COS1 cells (j, arrow). Localization of wild-type ezrin in actin-rich dorsal structures and mutated ezrin in cytoplasm is evident in xz sections. Bars, 10 μm.

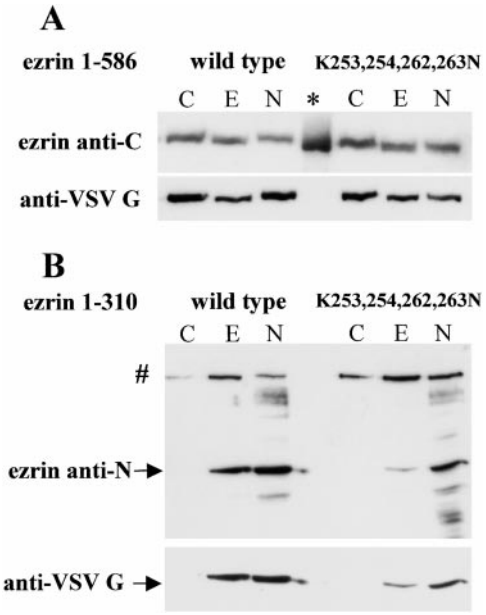

Figure 7. Subcellular localization of transfected mutated and wild-type ezrin in COS1 cells. Transfected cells were fractionated as described in Materials and Methods and the resulting fractions were analyzed by SDS-PAGE and immunoblotting. Before immunodecoration, blots were stained with Coomassie blue to ensure that protein loadings were comparable. (A) Transfection of full-length ezrin. Transfected VSV-tagged wild-type and K253N, K254N, K262N, and K263N (K253,254,262,263N) ezrin were recovered in cytosol (C), Triton X-100 extractable (E), or nonextractable (N) material, as revealed after immunoblotting with anti–VSV-G mAb. Anti-ezrin antibody, which recognizes both endogenous and VSV-G–tagged ezrin, was used as a control (top). *Internal control with recombinant wild-type ezrin (100 ng load). Results shown are representative of three independent experiments. (B) Transfection of ezrin 1-310. Detection of the top blot was performed with an antibody against the NH_2-terminal portion of ezrin. The proportion of cytosolic full-length ezrin (#) detected with this antibody is lower than that presented in A due to the poor accessibility of the anti–N antibody to the epitopes in the full-length ezrin. Note that some degradation of ezrin was detectable in the nonextractable material (N). Immunodetection of the bottom blot was performed with anti–VSV-G mAb.

Using the solid phase assay, we demonstrated that the three pair mutations (K > N; residues 63 and 64, 253 and 254, and 262 and 263) introduced in ezrin 1-333, either alone or in combination, did not impair its homotypic association with the full-length molecule (Fig. 4 D).

In addition, the intrinsic tryptophane fluorescence spectra of both wild-type ezrin and mutated molecule were similar upon normalization and exhibited identical maximum wavelength emission (Fig. 4 E). The 10% difference observed in the maximum intensity may be due to an overestimation of the protein concentration of wild-type ezrin, but in no case did the tryptophane fluorescence of the mutated ezrin appear to be significantly quenched upon exposure of trytophane(s) to solvent due to an inappropriate folding of the molecule.

Overall, the differences in the properties of wild-type and mutated ezrin documented in Fig. 4 are all very small, whereas the effects of the mutations on PIP_2 binding were drastic. The overall conformation of the ezrin molecule as well as some of its major functional binding properties appeared to be essentially preserved after introducing these mutations, except for its ability to interact with PIP_2-containing liposomes.

Alteration of the PIP_2-dependent Ezrin-CD44 Interaction

The interaction of ezrin with CD44 has been demonstrated to be PIP_2-dependent under physiological ionic strength conditions (Hirao et al., 1996). We therefore tested whether mutations in the residues involved in PIP_2 binding affected ezrin interaction with the cytoplasmic tail of CD44 in vitro. Indeed in the presence of PIP_2 micelles, the amount of wild-type ezrin binding to GST-CD44 immobilized on glutathione agarose beads was significantly increased (Fig. 5). In contrast, the binding of ezrin K253N, K254N, K262N, and K263N to the same beads was unaffected by PIP_2 addition, and was already comparable with the level obtained with wild-type ezrin in the presence of PIP_2. As a control, both the wild-type and mutated forms of ezrin did not bind to GST-glutathione agarose beads, irrespective of the presence of PIP_2 (Fig. 5).

Abnormal Localization of Ezrin Deficient in PIP_2 Binding

A431 epithelial cells and COS1 fibroblasts were transfected with ezrin K253N, K254N, K262N, and K263N or with wild-type ezrin, both constructs being tagged with VSV-G epitope. In A431 cells, wild-type ezrin VSV-G colocalized with F-actin at apical ruffles and microvilli, plasma membranes, and microspikes, as already described for endogenous ezrin (Gould et al., 1986; Algrain et al., 1993). Stress fibers and adhesive plaques were decorated with actin but not with ezrin (Fig. 6, a–c and g–i). On the contrary, in A431 and COS1 cells, mutated ezrin VSV-G was found to be located as a sponge-like network within the cytoplasm, clearly visible on single focal planes (Fig. 6, d and j) and xz sections. Mutated ezrin was only faintly detectable at the leading edge of plasma membranes or microspikes (Fig. 6 j). Clearly, mutated ezrin VSV-G labeling was excluded from vesicular structures. Expression of this mutated form of ezrin, however, did not alter cell size and morphology or actin-rich structures.

The subcellular distribution of wild-type and K253N, K254N, K262N, and K263N VSV-G–tagged ezrin was compared upon cell fractionation of COS1 cells. No marked difference was observed in partition of these proteins between cytosol and total membrane fractions (Fig. 7 A). However, the amount of Triton X-100 insoluble ezrin associated with the cytoskeleton was significantly lower in the case of mutated ezrin (37% of total cellular ezrin VSV-G vs. 27% of K253N, K254N, K262N, and K263N ezrin VSV-G; Fig. 7 A). As pointed out for actin, the distribution of endogenous ezrin was not significantly affected by expression of either form of ezrin VSV-G.

Loss of the Cell Extension Activity of the NH_2-Terminal Domain of Ezrin Upon Mutation of Its PIP_2 Binding Domain

COS1 fibroblasts were also transfected with the VSV-G–tagged NH_2-terminal domain of either wild-type or mutated ezrin. As previously described (Martin et al., 1997),

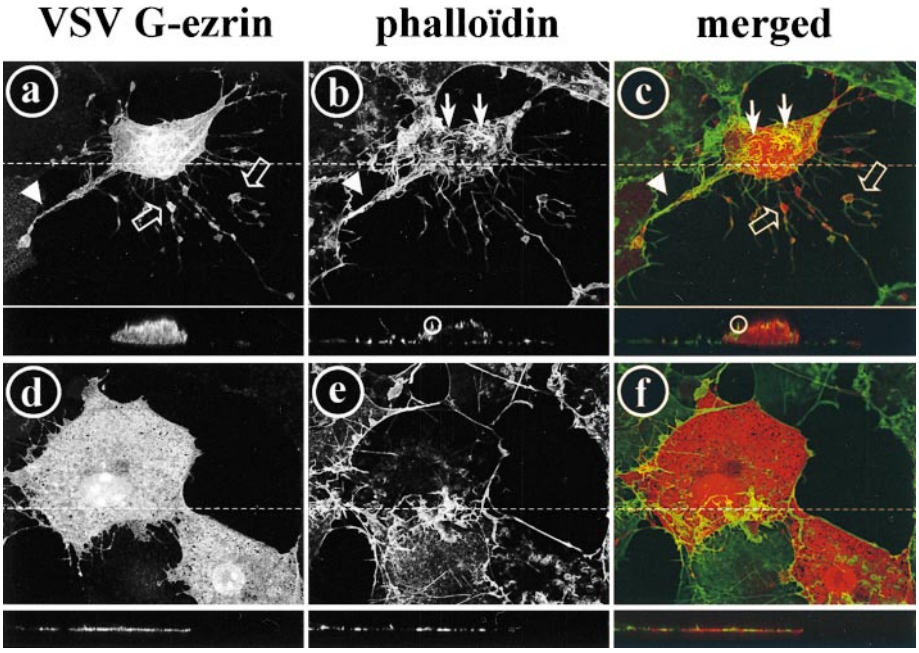

Figure 8. The mutated NH_2-terminal domain of ezrin partly loses its interactions with membranes. Monkey COS1 fibroblasts were transfected with either VSV-G–tagged wild-type (a–c) or mutated (K253N, K254N, K262N, and K263N) (d–f) ezrin 1-310 and treated for immunolocalization of actin (b and e) and VSV (a and d) as in Fig. 6. Transfected wild-type NH_2-terminal ezrin was mainly localized in actin-rich structures such as dorsal microvilli and ruffles (b and c, arrows; xz sections, circles). It induces formation of long filopodia containing both actin (b and c, arrowheads) and transfected ezrin (a and c, arrowheads). Note the presence of nodes along filopodia, particularly rich in NH_2-terminal ezrin (open arrows). The transfected mutated form of NH_2-terminal ezrin was predominantly localized in the cytoplasm (d and f), although some mutant ezrin localized in the same actin-rich structures (e and f) as wild-type NH_2-terminal ezrin. Staining of nuclei was observed only in cells transfected with mutated ezrin 1-310 (d and f). Bars, 10 μm.

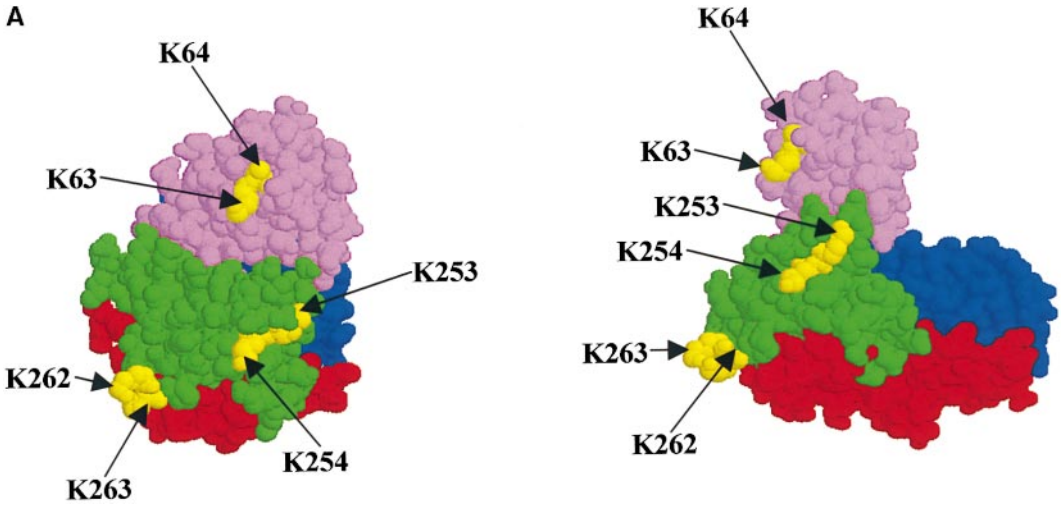

B MOESIN RESIDUES LOCATED AT THE INTERFACE WITH THE BILAYER

19 AIQ**PNTT**GK**Q**LFQ 31 (not applicable to merlin)

59 LKL**NKK**VS**A**QEV 70

243 SEI**RNIS**F**N**D**KK**FVI**K**PID**KK**AP**D**FVFYAPR**L**RIN**K**RIL 281

Q in radixin, D in merlin

Residues are different in merlin

D in ezrin and merlin

Figure 9. Location of the targeted lysines in moesin. The crystallographic data of moesin were treated with the molecular visualization program RASMOL (R. Sayle, Glaxo Wellcome, Greenford, UK). (A) The different domains of the molecule defined by Pearson et al. (2000) were colored as follows: residues 4–94, violet (domain FI); residues 95–201, blue (domain F2); residues 202–297, green (domain F3); and residues 488–577, red (COOH-terminal domain). The lysines of interest have been highlighted in yellow. The distances between the epsilon NH_2 of lysines 63–262, 63–254, and 254–263 are equal to 38.1, 27.6, and 19 Å, respectively. Note that all these lysines are accessible to solvent and therefore to PIP_2. They are all located on the same side of the molecule. (B) Moesin residues that may be in direct contact with the bilayer. Using RASMOL, residues exposed on the surface of moesin and enclosed by the triangle formed by lysines 63, 64, 253, 254, 262, and 263 (bold and underlined) have been identified (bold).

the transfection of the 1–310 fragment of ezrin induced formation of long filopodia, which contain both tagged ezrin 1-310 and actin (Fig. 8, a–c). This cell extension activity of the ezrin NH_2-terminal domain is dependent on the cell type used and was not observed in the case of CV1 cells (Algrain et al., 1993). Ezrin 1-310 and actin colocalized to a variable extent along these structures. Transfected ezrin 1-310 was also localized in actin-containing structures such as surface microvilli, dorsal ruffles, and lateral microspikes, comparable with the wild-type full-length molecule. Possibly due to its overexpression, tagged ezrin 1-310 was regularly observed in the cytoplasm and was excluded from vesicles. Strikingly, upon transfection of the cells with mutated ezrin 1-310, almost no cell extensions developed and the cells were extremely flattened. The localization of the mutated form of NH_2-terminal domain of ezrin appeared essentially cytoplasmic even if colabeling of some extensions containing actin persisted (Fig. 8, d–f). Note that with this construct some staining of the nucleoli was apparent (see Discussion). Upon cell fractionation, wild-type ezrin and mutated ezrin 1-310 were recovered in the particulate fraction (Fig. 7 B). At variance with the microscopic observations, no ezrin 1-310 was recovered in the cytosolic fraction. This discrepancy can be explained with the relative insolubility of the NH_2-terminal domains of ezrin, especially in low salt buffers such as those used for cell lysis.

Discussion

PIP_2, a lipid whose turnover is modified upon cell activation, has been implicated in the regulation of the functions of a number of cytoskeletal proteins (Janmey, 1995; Isenberg and Niggli, 1998). Depending on the protein studied, PIP_2 interactions may concentrate proteins at the plasma membrane in a manner affected by cell activation, possibly within PIP_2-enriched domains (Martin, 1998). PIP_2 may also modulate the function of the protein to which it binds (Gascard et al., 1993; Huttelmaier et al., 1998; Steimle et al., 1999). Knowledge of the molecular determinants involved in lipid–protein interactions is a prerequisite for studying their physiological role in intact cells. We have therefore analyzed the nature of PIP_2-binding determinants in ezrin by truncations, internal deletion, and site-directed mutagenesis. PIP_2 binding was studied using large liposomes containing 20% PIP_2 and 80% PC, in physiological salt concentrations. Presenting PIP_2 in mixed bilayers is much closer to the cellular environmental conditions than presentation as micelles of pure lipid. The advantage of the cosedimentation assays is also that free ezrin is always exposed to the bilayer and never separated during the assay. A disadvantage is that it cannot be completely excluded, that ezrin extracts some PIP_2 molecules to form a small complex that does not sediment. As previously shown, binding of full-length ezrin is maximal at ~20% PIP_2, and 5–10% of PIP_2 still induced significant association (Niggli et al., 1995). This is similarly the case for wild-type ezrin 1-333 (Fig. 3).

We first showed, by progressive truncations and internal deletions, that the NH_2 terminus of ezrin contains two domains essential for PIP_2 binding, located in regions 12–115 and 233–310. The loss of one of the sites resulted in almost complete loss of binding. Interestingly, recent findings for gelsolin similarly suggest that this protein binds to PIP_2-containing bilayers via a site formed by the juxtaposition of the NH_2- and COOH-terminal domains of gelsolin (Tuominen et al., 1999). To our knowledge, these are so far the only two proteins known with a pair of PIP_2-binding sites.

Inspection of the sequence of the NH_2-terminal domain of ezrin revealed two potential PIP_2 binding motifs, which are similar to the motifs identified in gelsolin and villin (Fig. 2). We have analyzed the role of these motifs in ezrin-PIP_2 binding by mutation of selected lysines to asparagines. These experiments revealed an important role of lysines 63 and 64, which are required for optimal binding. In contrast, two independent double mutations of lysines 253 and 254 or 262 and 263 to asparagines were of no consequence for the interaction with PIP_2. However, this does not mean that they are not involved in binding since mutation of all four lysines 253, 254, 262, and 263 resulted in an almost complete loss of binding similar to that observed after mutation of lysines 63, 64, 253, and 254. The presence of the lysines in the 63–72 motif is thus clearly necessary, but not sufficient for interaction. This conclusion is supported also by the inability of fragment 1–233 to bind to PIP_2. For optimal binding, the combined presence of K63, K64, K253, and K254 or K253, K254, K262, and K263 is thus required. Our results suggest that the two domains located in regions 63–72 and 253–263 do cooperate in PIP_2 binding. The site at amino acids 63–72 corresponds to a KKXXXXXX(K/R)K motif, which is similar to, but not identical with, the consensus sequence in villin, (K/R)XXXX(K/R)(K/R) (Yu et al., 1992). The site at amino acids 253–263, a KKXXXKXXXKK motif resembles a consensus sequence for gelsolin, (K/R)XXXKX(K/R)(K/R) (Yu et al., 1992). Typically, the motifs involved in ezrin–PIP_2 interaction start and end with two basic amino acids, whereas the sites in gelsolin and villin start with only one lysine or arginine. In addition, the numbers of interspersed amino acids are different in ezrin. Another motif has been detected in the cytoskeletal protein α-actinin, and also in spectrin and the PH domain of phospholipase C-δ1 and Grb7: RXXXXXXX(H/RK)XX(X)W(K/R) (Fukami et al., 1996). Again, this motif is not identical with those detected in ezrin.

During the completion of this manuscript, the crystal structure of a complex of the NH_2-terminal domain of moesin (residues 1–297) with the tail (residues 467–577) has been published (Pearson et al., 2000). According to this work, residues 63, 64, 253, 254, 262, and 263 are all located in loops connecting β sheets. In a space-filling model of moesin, the residues implicated in PIP_2 binding are all located on the surface of the molecule (Fig. 9 A). The residues form a triangle (Fig. 9 A). The surface enclosed by this triangle is relatively planar, so that a simultaneous contact of all residues with several PIP_2 molecules in a bilayer appears to be feasible. The residues enclosed by this triangle and exposed on the surface of moesin have been highlighted in the moesin sequence (Fig. 9 B). These residues, which could form a zone of contact with a PIP_2-containing bilayer, are identical in moesin and ezrin, with the exception of asparagine 62 in moesin, which corresponds to aspartic acid 62 in ezrin. Of these residues, including the lysines identified in this study, 36% are positively charged,

16% are negatively charged, 24% are uncharged but polar, and 24% are hydrophobic. Interestingly, Pearson et al. (2000) detected a hitherto unrecognized PH-like domain in the structural module F3 of moesin, where residues 253, 254, 262, and 263 are located. Such PH domains are involved in phosphoinositide binding and feature an antiparallel β sheet consisting of seven strands and a COOH-terminal α-helix (Harlan et al., 1995), comparable with the structure of F3 of moesin. Using the web-based tool SMART (Simple Molecular Architecture Research Tool; Schultz et al., 1998), we searched for a PH domain in the NH_2-terminal domain of ezrin, but were unsuccessful. If F3 indeed corresponds to a functional PH domain, then the distribution of charged amino acids is not typical for such domains. According to Pearson et al. (2000), the highly positively charged surface of lobe F3 of moesin may be suitable for binding of negatively charged phospholipids, in agreement with our results. Based on the crystallization results, the PIP_2 binding domain in ezrin is thus also different from the lipid-binding domain identified in vinculin, which has been shown to form an amphipathic helical hairpin (Johnson et al., 1998). Ezrin appears to contain two structural elements cooperating in PIP_2 binding and one of these elements may be part of a PH domain. These two domains do not appear to be directly involved in F-actin binding, nor do these mutations affect a distal F-actin binding site, as F-actin interaction of ezrin K253N, K254N, K262N, and K263N was not altered. A similar conclusion can be drawn for the interaction of ezrin with EBP 50.

It is unlikely that the effects reported in this paper on ezrin–PIP_2 interaction could be simply due to an overall change of the positive charges of the protein. For example, the double mutation K63N, K64N significantly decreased PIP_2 binding, whereas the two double mutations of lysines to asparagines at positions 253 and 254 or 262 and 263 had no significant effects. At pH 7.4, the calculated net global charge for the wild-type protein is +6.26 (ezrin 1-333) and −8.34 (ezrin 1-586). Introducing six K > N mutations yielded global charges that were +0.27 and −14.34. In spite of the net charge difference between ezrin 1-333 and full-length ezrin, the very same PIP_2-binding determinants were found to be important in the two molecules. Moreover, experiments were carried out under physiological ionic strength conditions. Under these conditions, the range of distances where electrostatics overcome thermal energies is relatively small, and the precise positioning of specific basic amino acids, rather than the overall charge of the NH_2-terminal domain, is likely to be important for ezrin–PIP_2 interaction. For example, the PH domain of pleckstrin is electrically polarized (Blomberg and Nilges, 1997), and mutation of three conserved lysine residues in this domain has been shown to result in 10-fold decrease in lipid-binding affinity (Harlan et al., 1995). As outlined for the PH domain, other determinants for PIP_2 interaction, based, for example, on interactions with acyl chains of the lipid, exist and may account for a pronounced, albeit incomplete, loss in affinity as described in the case of the mutated PH domain of pleckstrin (Harlan et al., 1995).

Interestingly, the introduction of two double mutations (K253N, K254N and K262N, K263N) results in the loss of PIP_2 requirement for optimal binding of ezrin to the cytoplasmic tail of CD44. As shown in Fig. 5, the binding between CD44 and the mutated form of ezrin is not impaired but becomes PIP_2 independent. This portion of the CD44 molecule contains clusters of basic amino acids involved in the CD44/ezrin interaction (Legg and Isacke, 1998). PIP_2 may neutralize basic residues in ezrin, resulting in elimination of repulsive forces between the two molecules. Introducing the mutations may generate the same effect. However, using truncation experiments, Yonemura et al. (1998) demonstrated that the first 19 residues of the cytoplasmic tail of CD44, containing a cluster of basic residues, were sufficient, at physiological ionic strength, to allow ERM-CD44 interactions, whereas binding of the full-length cytoplasmic tail was markedly reduced under these conditions. These interactions were studied in the absence of PIP_2. This finding cannot be reconciled with the hypothesis that charge neutralization by lipid is required for such a protein interaction to occur.

Wild-type VSV-G–tagged ezrin is massively recruited to dorsal actin-rich structures. The K253N, K254N, K262N, and K263N mutated form of ezrin was introduced into both epithelioid and fibroblastic cell lines. Immunofluorescence localization showed that the VSV-G–tagged mutant was now mainly located in the cytoplasm, without colocalization with F-actin and only weak binding to plasma membranes. Based on our in vitro findings, one would expect that mutated ezrin would bind to plasma membrane proteins independently of PIP_2. In fact, Legg and Isacke (1998) concluded, using CD44-negative cells, that the localization of ezrin to microvilli was not mediated through an interaction with CD44, but rather with other sites at which the actin network closely associated with the plasma membrane. In our study, mutated ezrin expressed in cells no longer localizes to microvilli and ruffles, suggesting that a direct PIP_2–ezrin interaction may be one of the necessary events to address ezrin to these specific membrane structures. Since ERM proteins are involved in the formation of the very same structures, the cytoplasmic localization of the mutated ezrin protein might simply result from an upstream defect (PIP_2 binding) absolutely required for the formation of a novel ezrin-containing membrane structure. Cell fractionation studies showed indeed that recovery of the mutated ezrin in the cytoskeleton-associated membrane fraction was significantly reduced as compared with the wild-type protein, supporting the immunofluorescence studies. However, total recovery in the membrane fraction appeared not to be altered. This may be due to redistribution occurring during the isolation procedure using detergent.

It has been suggested that multimeric forms of ezrin are involved in the generation of actin-rich structures (Gary and Bretscher, 1993). Interactions between NH_2-terminal domains of ERM proteins and full-length proteins resulting in multimer formation have been shown to interfere with the normal functions of endogenous proteins in the NIH3T3 cell line (Henry et al., 1995; Amieva et al., 1999). Using a solid phase assay, we found that wild type as well as mutated ezrin 1-333 and full-length ezrin engaged in homotypic interactions (Fig. 4 D). However, by immunolocalization, no mutated ezrin was found associated with actin-rich structures. We can thus conclude that the formation of heterodimers of wild-type and mutated ezrin is not sufficient for the association with actin-containing domains.

A number of reasons led us to transfect cells with the whole NH_2-terminal domain of ezrin (residues 1–310) rather than the portion of the protein containing the PIP_2 binding determinants (residues 63–263). Amino acids beyond 296 are necessary for engaging in homotypic as well as heterotypic interactions (Gary and Bretscher, 1993). Deletion of amino acids 13–30 in ezrin (Martin et al., 1997) or of the first 11 residues of moesin (Amieva et al., 1999) led to drastic changes of the localization of the NH_2-terminal portion of these proteins. Ezrin 1-320 still localizes to the membrane, whereas fragment 1-276 is cytosolic (Amieva et al., 1999). Thus, deleting any of these portions of the molecule may be dominant over the mutations of the PIP_2 binding determinants. In fact, introduction of the latter mutations led to an expression pattern similar to the one observed for any of the deletions described above. These observations suggest that any change in the NH_2-terminal domain of the ERM can drastically affect the protein structure and/or function. Of interest is the observation that when the PIP_2 binding determinants were mutated, the NH_2-terminal domain of ezrin localized within the nucleoli. Although the possibility of an artifact has to be considered, a 55-kD ezrin-related protein that cross-reacts with antibodies against the NH_2-terminal domain of ezrin has been detected in the nucleus of many human transformed cells (Kaul et al., 1999). Evidence has also been presented for the nuclear localization of isoforms of protein 4.1, the first member of the ERM family (Correas, 1991). In this latter case, at variance with our observations, a cluster of basic residues was necessary for such a localization to occur (Luque et al., 1998).

In conclusion, two PIP_2 binding determinants exist in ezrin in regions 12-115 and 233-310 of the protein, with lysines 63, 64, 253, 254, 262, and 263 playing a major role for efficient interaction. As these residues are conserved in the ERM family (Fig. 2), ezrin, moesin, and radixin may specifically bind to PIP_2 using the same determinants. Although we cannot exclude the possibility that the mutations described in this work alter other functions of ezrin, these mutated residues are likely candidates involved in the targeting of ezrin to, and presumably in the formation of, F-actin–rich membrane structures.

We thank Kathy Mujynya Ludunge and Christelle Anguille for excellent technical assistance, Professor H.U. Keller for continuous support, Dr. E. Sigel for critical reading of the manuscript, and Sabine Baumann for helpful discussions. We are most grateful to Drs. M. Arpin, A. Bretscher, and R. Lamb for generous sharing of materials.

This work was supported by the Centre National de la Recherche Scientifique (Cell Biology project 96033 to C. Roy), by l'Association pour la Recherche sur le Cancer (to P. Mangeat, C. Roy, and C. Barret), by la Ligue Nationale contre le Cancer and la Fondation pour la Recherche Médicale (to C. Barret), and by the Swiss National Foundation for Scientific Research (grant 31-49197.96 to V. Niggli).

Submitted: 16 May 2000
Revised: 6 October 2000
Accepted: 12 October 2000

Note added in proof. During revision of this manuscript, K. Hamada and colleagues published the crystal structure of radixin complexed to inositol-(1,4,5)-triphosphate (IP3) (Hamada, K., T. Shimizu, T. Matsui, Sh. Tsukita, Sa. Tsukita, and T. Hakoshima. 2000. *EMBO (Eur. Mol. Biol. Organ.) J.* 19:4449–4462). Most other residues identified in our study are in the vicinity of IP3.

References

Algrain, M., O. Turunen, A. Vaheri, D. Louvard, and M. Arpin. 1993. Ezrin contains cytoskeleton and membrane binding domains accounting for its proposed role as a membrane-cytoskeletal linker. *J. Cell Biol.* 120:129–139.

Amieva, M.R., P. Litman, L. Huang, E. Ichimaru, and H. Furthmayr. 1999. Disruption of dynamic cell surface architecture of NIH3T3 fibroblasts by the N-terminal domains of moesin and ezrin: in vivo imaging with GFP fusion proteins. *J. Cell Sci.* 112:111–125.

Andréoli, C., M. Martin, R. Leborgne, H. Reggio and P. Mangeat. 1994. Ezrin has properties to self-associate at the plasma membrane. *J. Cell Sci.* 107: 2509–2521.

Blomberg, N., and M. Nilges. 1997. Functional diversity of PH domains: an exhaustive modelling study. *Fold. Des*. 2:343–355.

Bradford, M.M. 1976. A rapid and sensitive method for the quantitation of microgram quantities of protein utilizing the principle of protein-dye binding. *Anal. Biochem*. 72:248–254.

Bretscher, A. 1999. Regulation of cortical structure by the ezrin-radixin-moesin protein family. *Curr. Opin. Cell Biol*. 11: 109–116.

Correas, I. 1991. Characterization of isoforms of protein 4.1 in the nucleus. *Biochem. J*. 279:581–585.

Flanagan, L.A., C.C. Cunningham, J. Chen, G.D. Prestwich, K.S. Kosik and P.A. Janmey. 1997. The structure of divalent cation-induced aggregates of PIP_2 and their alteration by gelsolin and tau. *Biophys. J*. 73:1440–1447.

Franck, Z., R. Gary, and A. Bretscher. 1993. Moesin, like ezrin, colocalizes with actin in the cortical cytoskeleton in cultured cells, but its expression is more variable. *J. Cell Sci.* 105:219–231.

Fukami, K., N. Sawada, T. Endo, and T. Takenawa. 1996. Identification of a phosphatidylinositol 4,5-bisphosphate binding site in chicken skeletal muscle alpha-actinin. *J. Biol. Chem*. 271:2646–2650.

Gary, R., and A. Bretscher. 1993. Heterotypic and homotypic associations between ezrin and moesin, two putative membrane-cytoskeletal linking proteins. *Proc. Natl. Acad. Sci. USA*. 90:10846–10850.

Gascard, P., G.P. Pawelczyk, J.M. Lowenstein, and C.M. Cohen. 1993. The role of inositol phospholipids in the association of band 4.1 with the human erythrocyte membrane. *Eur. J. Biochem.* 211:671–681.

Gautreau, A., P. Poullet, D. Louvard, and M. Arpin. 1999. Ezrin, a plasma membrane-microfilament linker, signals cell survival through the phosphatidylinositol 3-kinase/Akt pathway. *Proc. Natl. Acad. Sci. USA*. 96:7300–7305.

Gould, K.L., J.A. Cooper, A. Bretscher, and T. Hunter. 1986. The protein-tyrosine substrate, p81, is homologous to a chicken microvillar core protein. *J. Cell Biol.* 102:660–669.

Harlan, J.E., H.S. Yoon, P.J. Hajduk, and S.W. Fesik. 1995. Structural characterization of the interaction between a pleckstrin homology domain and phosphatidylinositol 4,5-bisphosphate. *Biochemistry*. 34:9859–9864.

Heiska, L., K. Alfthan, M. Grönholm, P. Vilja, A.Vaheri, and O. Carpèn. 1998. Association of ezrin with intercellular adhesion molecule-1 and -2 (ICAM-1 and ICAM-2). Regulation by phosphatidylinositol 4,5-bisphosphate. *J. Biol. Chem*. 273:21893–21900.

Henry, M.D., C. Gonzalez Agosti, and F. Solomon. 1995. Molecular dissection of radixin: distinct and interdependent functions of the amino- and carboxy-terminal domains. *J. Cell Biol.* 129:1007–1022.

Hirao, M., N. Sato, T. Kondo, S. Yonemura, M. Monden, T. Sasaki, Y. Takai, S. Tsukita, and S. Tsukita. 1996. Regulation mechanism of ERM (ezrin/radixin/moesin) protein/plasma membrane association: possible involvement of phosphatidylinositol turnover and Rho-dependent signaling pathway. *J. Cell Biol.* 135:37–51.

Huttelmaier, S., O. Mayboroda, B. Harbeck, T. Jarchau, B.M. Jockusch, and M. Rudiger. 1998. The interaction of the cell-contact proteins VASP and vinculin is regulated by phosphatidylinositol-4,5-bisphosphate. *Curr. Biol.* 8:479–488.

Isenberg, G., and V. Niggli. 1998. Interaction of cytoskeletal proteins with membrane lipids. *Int. Rev. Cytol.* 178:73–125.

Janmey, P.A. 1995. Protein regulation by phosphatidylinositol lipids. *Chem. Biol.* 2:61–65.

Janmey, P.A., J. Lamb, P.G. Allen, and P.T. Matsudaira. 1992. Phosphoinositide-binding peptides derived from the sequences of gelsolin and villin. *J. Biol. Chem*. 267:11818–11823.

Johnson, R.P., V. Niggli, P. Durrer, and S.W. Craig. 1998. A conserved motif in the tail domain of vinculin mediates association with and insertion into acidic phospholipid bilayers. *Biochemistry*. 37:10211–10222.

Kaul, S.C., R. Kawai, H. Nomura, Y. Mitsui, R.R. Reddel, and R. Wadhwa. 1999. Identification of a 55 kDa ezrin-related protein that induces cytoskeletal changes and localizes to the nucleolus. *Exp. Cell Res.* 250:51–61.

Kreis, T.E. 1986. Microinjected antibodies against the cytoplasmic domain of vesicular stomatitis virus glycoprotein block its transport to the cell surface. *EMBO (Eur. Mol. Biol. Organ.) J.* 5:931–941.

Legg, J.W., and C.M. Isacke. 1998. Identification and functional analysis of the ezrin-binding site in the hyaluronan receptor CD44. *Curr. Biol.* 8:705–708.

Luque, C.M., M.J. Lallena, M.A. Alonso, and I. Correas. 1998. An alternative domain determines nuclear localization in multifunctional protein 4.1. *J. Biol. Chem*. 273:11643–11649.

Mangeat, P., C. Roy, and M. Martin. 1999. ERM proteins in cell adhesion and membrane dynamics. *Trends Cell Biol.* 9:187–192.

Martin, T.F.J. 1998. Phosphoinositide lipids as signaling molecules: common themes for signal transduction, cytoskeletal regulation, and membrane trafficking. *Annu. Rev. Cell. Dev. Biol.* 14:231–264.

Martin, M., C. Roy, P. Montcourrier, A. Sahuquet, and P. Mangeat. 1997. Three determinants in ezrin are responsible for cell extension activity. *Mol. Biol. Cell.* 8:1543–1557.

Matsui, T., S. Yonemura, Sh. Tsukita and Sa. Tsukita. 1999. Activation of ERM proteins *in vivo* by Rho involves phosphatidyl-inositol 4-phosphate 5-kinase and not ROCK kinases. *Curr. Biol.* 9:1259–1262.

Murthy, A., C. Gonzalez Agosti, E. Cordero, D. Pinney, C. Candia, F. Solomon, J. Gusella, and V. Ramesh. 1998. NHE-RF, a regulatory cofactor for Na^+–H^+ exchange, is a common interactor for merlin and ERM (MERM) proteins. *J. Biol. Chem*. 273:1273–1276.

Nakamura, F., L. Huang, K. Pestonjamasp, E. Luna, and H. Furthmayr. 1999. Regulation of F-actin binding to platelet moesin in vitro by both phosphorylation of threonine 558 and polyphosphoinositides. *Mol. Biol. Cell*. 10:2669–2685.

Niggli, V., C. Andréoli, C. Roy, and P. Mangeat. 1995. Identification of a phosphatidylinositol-4,5-bisphosphate–binding domain in the NH_2-terminal region of ezrin. *FEBS Lett.* 376:172–176.

Niggli, V., S. Kaufmann, W.H. Goldmann, T. Weber, and G. Isenberg. 1994. Identification of functional domains in the cytoskeletal protein talin. *Eur. J. Biochem*. 224:951–957.

Pearson, M.A., D. Reczek, A. Bretscher, and P.A. Karplus. 2000. Structure of the ERM protein moesin reveals the FERM domain fold masked by an extended actin binding tail domain. *Cell*. 101:259–270.

Reczek, D., M. Berryman, and A. Bretscher. 1997. Identification of EBP50: a PDZ-containing phosphoprotein that associates with members of the ezrin-radixin-moesin family. *J. Cell Biol.* 139:169–179.

Roy, C., M. Martin, and P. Mangeat. 1997. A dual involvement of the amino-terminal domain of ezrin in F- and G-actin binding. *J. Biol. Chem*. 272:20088–20095.

Schultz, J., F. Milpetz, P. Bork, and C.P. Ponting. 1998. SMART, a simple modular architecture research tool: identification of signaling domains. *Proc. Natl. Acad. Sci. USA*. 95:5857–5864.

Serrador, J.M., J.L. Alonso Lebrero, M.A. del Pozo, H. Furthmayr, R. Schwartz Albiez, J. Calvo, F. Lozano, and F. Sanchez Madrid. 1997. Moesin interacts with the cytoplasmic region of intercellular adhesion molecule-3 and is redistributed to the uropod of T lymphocytes during cell polarization. *J. Cell Biol.* 138:1409–1423.

Short, D.B., K.W. Trotter, D. Reczek, S.M. Kreda, A. Bretscher, R.C. Boucher, M.J. Stutts, and S.L. Milgram. 1998. An apical PDZ protein anchors the cystic fibrosis transmembrane conductance regulator to the cytoskeleton. *J. Biol. Chem*. 31:19797–19801.

Steimle, P.A., J.D. Hoffert, N.B. Adey, and S.W. Craig. 1999. Polyphosphoinositides inhibit the interaction of vinculin with actin filaments. *J. Biol. Chem*. 274:18414–18420.

Tuominen, E.K.J., J.M. Holopainen, J. Chen, G.D. Prestwich, P.R. Bachiller, P.K.J. Kinnunen, and P.A. Janmey. 1999. Fluorescent phosphoinositide derivatives reveal specific binding of gelsolin and other actin regulatory proteins to mixed lipid bilayers. *Eur. J. Biochem.* 263:85–92.

Yonemura, S., M. Hirao, Y. Doi, N. Takahashi, T. Kondo, S. Tsukita, and S. Tsukita. 1998. Ezrin/radixin/moesin (ERM) proteins bind to a positively charged amino acid cluster in the juxta-membrane cytoplasmic domain of CD44, CD43, and ICAM-2. *J. Cell Biol.* 140:885–895.

Yu, F.-X., H.-Q. Sun, P. Janmey, and H.L. Yin. 1992. Identification of a polyphosphoinositide-binding sequence in an actin monomer-binding domain of gelsolin. *J. Biol. Chem*. 267:14616–14621.

Yun, C.H.C., G. Lamprecht, D.V. Forster, and A. Sider. 1998. NHE3 kinase A regulatory protein E3KARP binds the epithelial brush border Na^+/H^+ exchanger NHE3 and the cytoskeletal protein ezrin. *J. Biol. Chem*. 273:25856–25863.